Journal of Alloys and Compounds 508 (2010) 396–399

Contents lists available at ScienceDirect

Journal of Alloys and Compounds

journal homepage: www.elsevier.com/locate/jallcom

The preparation and characterization of Ni–Fe bioxide composite nanoparticles

Qingmei Zhang, Jian Li*, Yueqiang Lin, Xiaodong Liu, Hua Miao

School of Physical Science & Technology, MOE Key Laboratory on Luminescence and Real-Time Analysis, Southwest University, Tianshenglu Road, Chongqing 400715, People's Republic of China

ARTICLE INFO

Article history:
Received 13 April 2010
Received in revised form 2 August 2010
Accepted 16 August 2010
Available online 26 August 2010

Keywords:
Co-precipitation
Oxide
Composite
Nanoparticles
$FeCl_2$ solution

ABSTRACT

Using co-precipitation and processing in $FeCl_2$ solution, Ni–Fe bioxide composite nanoparticles have been prepared. The precursor and the as-prepared nanoparticles are characterized by TEM, XRD, EDX, XPS and VSM. The precursor, consisting of a mixture of FeOOH and $Ni(OH)_2$, has been synthesized using the well-known co-precipitation method. Using heat treatment in $FeCl_2$ solution, at 100 °C, in atmosphere and autoclave, a transition took place in which in addition to the $Ni(OH)_2$ partially dissolving, the precursor was transformed into Ni_2O_3–Fe_2O_3 composite nanoparticles of about 10 nm diameter. The transition in $FeCl_2$ solution denoted a transition induced chemical reaction, which is different from the transition induced thermally by calcination technology. In the chemically induced transition, following the dehydration, there is no diffusion of metal ions, as would arise from a thermally induced transition but there is local migration of metal ions to form grains. The chemically induced transition in $FeCl_2$ solution can be part of a new route for the preparation of composite or single phase oxide nanoparticles by the co-precipitation method.

1. Introduction

Magnetic nanoparticles, with sizes ranging from 2 to 20 nm in diameter, represent an important class of artificial nanostructured materials and have attracted increasing interest in the field of basic science and for their technological applications in electronic, optoelectronic and spintronic devices [1,2]. Studies of magnetic nanoparticles have been focussed on the development of novel synthetic technology [3]. A nanocomposite is a material composed of two or more phases, one of which has a grain size of less than 100 nm. The combination of different physical or chemical properties may lead to completely novel materials [4]. A few bimetallic composite nanoparticles, such as Fe–Pt, Pt–Rh, Pd–Pt, Ag–Au and Au–Pd nanoparticles, have been prepared [1,5–8]. In recent years, composite nanoparticles based on oxides, such as metallic-oxide composite nanoparticles of Au–γ-Fe_2O_3, Au–Fe_3O_4 [9], polymer-oxide composite nanoparticles of PPy–γ-Fe_2O_3 [10], PPA–γ-Fe_2O_3 [4] and bioxide composite nanoparticles of γ-Fe_2O_3–SiO_2, Fe_3O_4–SiO_2 [3,11,12], have also been prepared. Magnetic nanocomposites have applications ranging from ferrofluids to separation science and technology [13]. In the present work, bioxide composite nanoparticles based both on Ni_2O_3, which has a sewage disposal function, and ferrimagnetic γ-Fe_2O_3 were prepared by treating the precursor in $FeCl_2$ solution in atmosphere or autoclave. The morphology, crystal structure, chemical components and magnetization were characterized for both the precursor and nanoparticles. Accordingly, a mechanism for the transition of the precursor into the bioxide composite nanoparticles is proposed.

2. Experimental

2.1. Preparation

The preparation of the nanoparticles can be divided into two steps. First, the precursor was synthesized using the co-precipitation method. An aqueous mixture of $FeCl_3$ (40 ml, 1 M) and $Ni(NO_3)_2$ (10 ml, 2 M, in HCl 0.05 mol) in which the ratio of Fe^{3+} to Ni^{2+} was 2:1 was added to NaOH solution (500 ml, 0.7 M). Then the solution was heated to boiling point for 5 min with stirring. After the heating was stopped, the black precursor was gradually precipitated. It was then washed with a low concentration of HNO_3 solution (0.01 M) to pH = 7–8.

The second step was to obtain the composite nanoparticles by two methods. The first method was to add the precursor to $FeCl_2$ solution (0.25 M) to obtain 400 ml of mixture solution. Then the mixture solution was heated to boiling for 30 min in atmosphere, and the nanoparticles were precipitated gradually after the heating stopped (denoted as treated sample (1)). The other way was to add the precursor to $FeCl_2$ solution (0.25 M) to obtain 200 ml of the mixture solution. Then the mixture solution was put into the autoclave, heated to 100 °C for 1 h and cooled to room temperature naturally (denoted as treated sample (2)). Finally, these particles were dehydrated with acetone and allowed to dry naturally. For comparison, $NiFe_2O_4$ particles were prepared by calcination of the precursor at 850 °C for 2 h in air, which is called the calcined sample.

2.2. Characterization

To investigate the transition process from the precursor to the particles, both precursor and treated samples were characterized. The morphology, crystal structure, size and chemical composition of the samples were analyzed using transmission electron microscopy (TEM, PHLIPS TECNAI 10, at 100 kV), X-ray diffraction

* Corresponding author.
E-mail address: aizhong@swu.edu.cn (J. Li).

0925-8388/$ – see front matter.
doi:10.1016/j.jallcom.2010.08.065

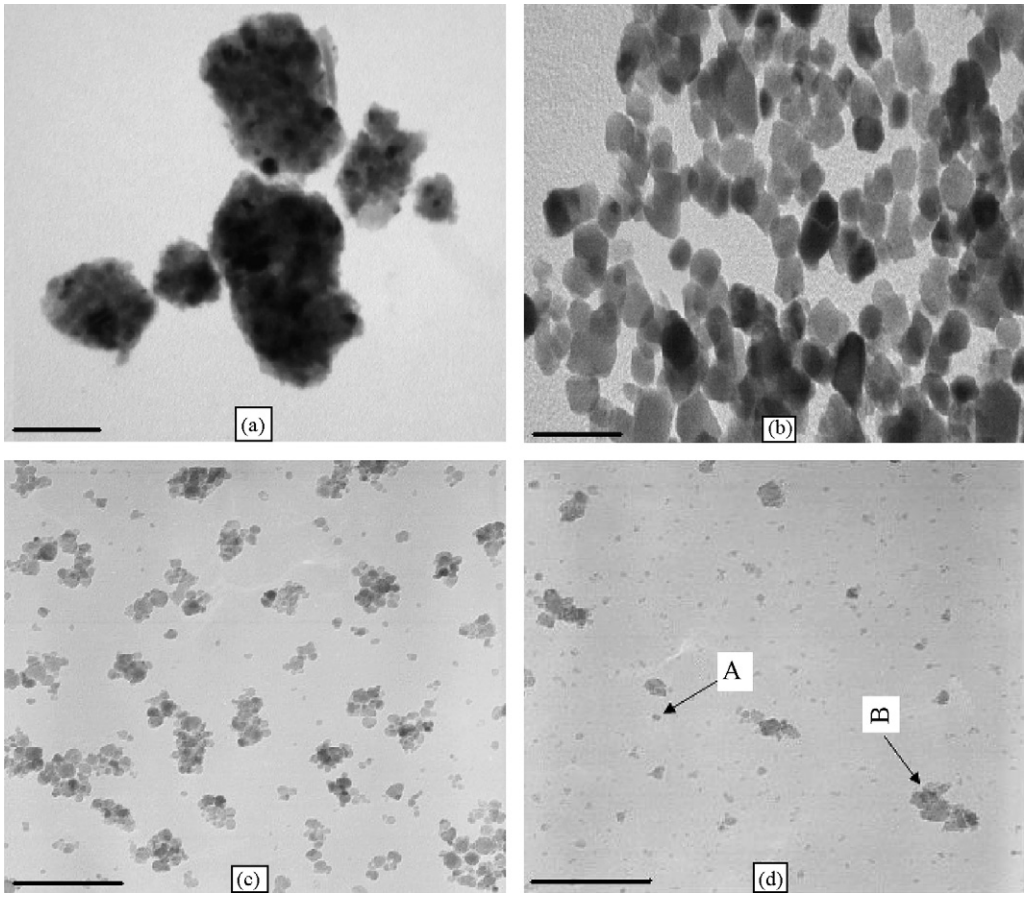

Fig. 1. TEM images of (a) the precursor, (b) the calcined sample, (c) the treated sample (1) and (d) the treated sample (2). The size bars are 100 nm.

(XRD, XD-2, CuKα radiation), energy dispersive X-ray spectroscopy (EDX, Norton 8000, at 25 kV) and X-ray Photoelectron Spectroscopy (XPS, Thermo ESCA 250, Mg target). A vibrating sample magnetometer (VSM, ADE EV-11, applied magnetic field up to 2×10^4 Oe) was used to measure the magnetization of the samples at room temperature. The calcined sample is characterized by TEM, EDX and XPS.

3. Results and analysis

TEM observations of the samples are shown in Fig. 1. These reveal that the precursor is loosely aggregated, and the sizes of the treated samples are far less than those of the calcined sample. The shapes of the particles in the treated samples (1) are nearly spherical and the size is about 10 nm. The treated sample (2) formed aggregates with different sizes (as indicated by arrow B) in addition to particles of about 10 nm diameter (as indicated by arrow A). They also exhibited poorer dispersity than sample (1).

Fig. 2 displays the XRD patterns for the precursor and the two treated samples. The results indicate that the precursor is amorphous, and the treated samples mainly contained γ-Fe_2O_3 with a much weaker Ni_2O_3 trace. For ferrite nanoparticles, the grain sizes d can be estimated from the half-maximum width of the (3 1 1) diffraction peak β by Scherrer's formula [14]: $d = k\lambda/\beta \cos\theta$, where k is constant, 0.98, λ is wavelength of the X-ray (Cu Kα = 0.1542 nm) and θ is the Bragg diffraction angle of (3 1 1) plane. Thus, the γ-Fe_2O_3 grain sizes of the treated samples (1) and (2) can be calculated from the (3 1 1) diffraction peak as 8.1 and 7.7 nm, respectively.

EDX analysis showed that the precursor and the calcinated sample were made up of Ni and Fe, but the treated samples contained some Cl as well. Quantitative analysis showed that the mole ratios of Ni to Fe in the precursor and the calcinated sample are about 1:2, which is the same as that of the starting reagents, but the ratio in the samples treated in atmosphere and autoclave are only about 0.17:2 and 0.22:2, respectively. The detailed data are listed in Table 1. In addition, for the treated samples (1) and (2), the concentrations of Cl are only about 3% and 1%, respectively. The detailed data are given in Table 2.

The XPS results indicated that the precursor consisted of Ni, Fe and O and the treated samples contained some additional Cl. It was found by quantitative analysis that the ratio of Ni to Fe in the precur-

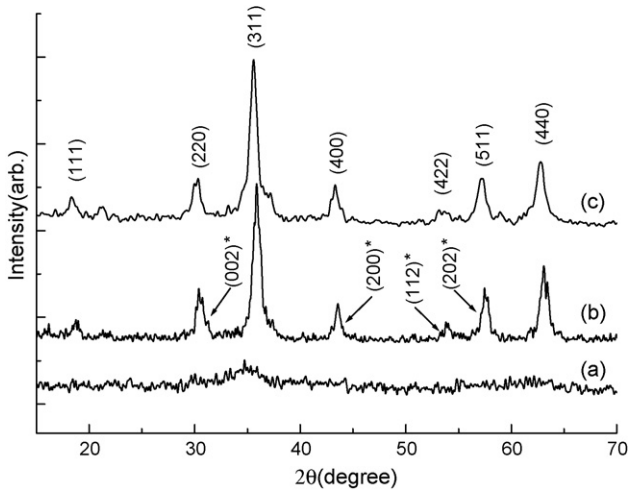

Fig. 2. XRD patterns of (a) the precursor, (b) the treated sample (1) and (c) the treated sample (2). (·) Corresponds to the diffraction peaks of γ-Fe_2O_3 and (·)* Corresponds to the diffraction peaks of Ni_2O_3.

Table 1
The ratios of Ni to Fe (at%) from EDX and XPS measurements.

	EDX		XPS	
	Ni	Fe	Ni	Fe
The precursor	33.4	66.6	44.8	55.2
The calcinated sample	32.4	67.6	34.4	65.6
The treated sample (1)	7.8	92.2	11.4	88.6
The treated sample (2)	10.0	90.0	26.5	73.6

Table 2
The atomic percentages of Fe, Ni and Cl from EDX and XPS measurements.

		Fe	Ni	Cl
The treated sample (1)	EDX	89.4	7.6	3.0
	XPS	73.3	9.4	17.3
	XPS/EDX	0.8	1.2	5.8
The treated sample (2)	EDX	89.0	9.9	1.1
	XPS	66.5	23.9	9.6
	XPS/EDX	0.8	2.4	8.7

sor is greater than 1:2, in the treated samples using $FeCl_2$ solution much less than 1:2, and for the calcined sample is about 1:2, the same result as the EDX, as listed in Table 1. In addition, the content of Cl in the treated sample (2) is less than in the treated sample (1), as listed in Table 2. The values of the binding energies showed that the precursor consisted of both FeOOH and $Ni(OH)_2$, and the treated sample consisted of Fe_2O_3, Ni_2O_3 and $FeCl_3$. It is noted that the binding energies of Ni2p and O1s for both $Ni(OH)_2$ and Ni_2O_3 are very close. However, $Ni(OH)_2$ would be dissolved in the treatment with $FeCl_2$ solution. Accordingly, the phase is Ni_2O_3 rather than $Ni(OH)_2$ in the treated samples. This also agrees with the XRD result. The complete data are listed in Table 3.

Fig. 3 shows the magnetization curves of the samples. Clearly, the precursor is apparently paramagnetic and the other two samples are ferrimagnetic. The specific saturation magnetization σ_s of the ferromagnetic samples can be estimated from the linear relationship between σ and $1/H$ at high field [15]. For the particles prepared in atmosphere and autoclave, these values are 71.81 and 62.59 emu/g, respectively.

4. Discussion

The results show that the precursor is an amorphous composite of FeOOH and $Ni(OH)_2$. Since the ratio of Ni to Fe measured by XPS is larger than that of the starting reagents yet the EDX measurement is in agreement, it is concluded that the $Ni(OH)_2$ species has formed outside the FeOOH species in the precursor, since the XPS information comes from the surface layer, less than 3 nm thick, but

Table 3
Binding energy data for the elements of the precursor, the calcinated sample and the treated samples from XPS (eV).

	Fe2p	Ni2p	O1s	Cl2p
The precursor	711.15	855.81	530.75	
FeO*O**H	711.40		*530.10	
			**531.20	
$Ni(OH)_2$		855.80	531.50	
The treated sample (1)	711.05	855.79	530.63	198.45
The treated sample (2)	711.13	855.32	530.16	198.32
γ-Fe_2O_3	710.90		529.80	
Ni_2O_3		855.60	531.80	
$FeCl_3$	711.10			198.80

Note: The standard data for FeO*O**H, $Ni(OH)_2$, γ-Fe_2O_3, Ni_2O_3 and $FeCl_3$ are taken from the PHI 5300 ESCA Data Bank and the Handbook of X-ray Photoelectron Spectroscopy. O* and O** mean the oxygen elements of different position in FeOOH compounds.

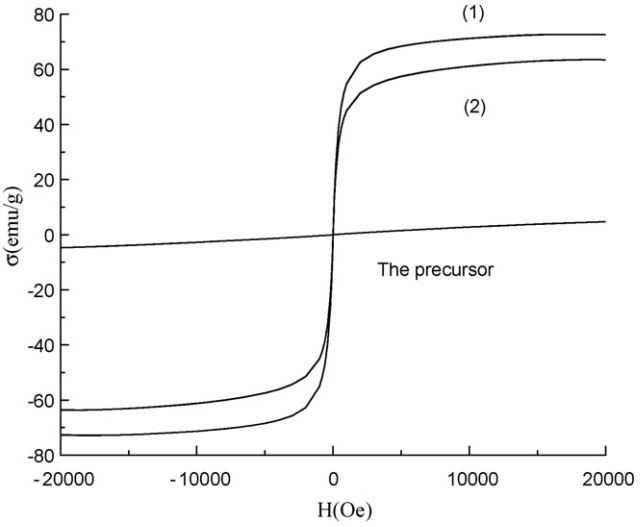

Fig. 3. The magnetization curves of the (a) precursor, (b) the treated sample (1) and (c) the treated sample (2).

the EDX information comes from a depth of about 1 μm. The analysed results of the calcined sample confirm that when the chemical species are uniformly distributed in the particles, e.g. the $NiFe_2O_4$ nanoparticles, the results of both EDX and XPS analysis should be about the same.

The results of the analysis show that when the amorphous precursor consisting of FeOOH and $Ni(OH)_2$ was thermally treated in $FeCl_2$ solution, a transition took place to form Ni–Fe oxide composite nanoparticles as well as partial dissolution of the $Ni(OH)_2$ species. Clearly, the dehydration reaction also takes place in $FeCl_2$ solution in the same way as during the calcination process. The schematic reaction in $FeCl_2$ solution can be written as

$$2FeOOH \rightarrow \gamma\text{-}Fe_2O_3 + H_2O$$

$$4Ni(OH)_2 + O_2 \rightarrow 2Ni_2O_3 + 4H_2O$$

These means that, for the transition induced in $FeCl_2$ solution, there is no diffusion of metal ions but only local migration to form the γ-Fe_2O_3 and Ni_2O_3. In addition, the partial dissolution of $Ni(OH)_2$ can increase the pH value of the solution, which could assist precipitation. Obviously, the dissolution of $Ni(OH)_2$ in the autoclave is more difficult than in atmosphere, so that the Ni_2O_3 content in the treated sample (2) is higher than that of the treated sample (1). From the differences in the ratios of Ni, Fe, and Cl found by EDX and XPS measurements for the treated samples (see Table 2), it can be judged that the core consists of γ-Fe_2O_3, Ni_2O_3 is formed outside the γ-Fe_2O_3 and the outermost layer of the particles absorb $FeCl_3$, which results from the oxidization of $FeCl_2$. This is concluded from the XPS measurement, since the nearer to the sample surface, the larger is the deviation of the ratio of the chemical species from the real ratio in the total sample. The real ratio is described by the EDX results. Thus, the synthesis of the nanoparticles by co-precipitation and processing in $FeCl_2$ solution follow the scheme shown in Fig. 4. In addition, the migration of ions in the autoclave is more difficult than in atmosphere, so that the grains are fewer and the dispersity is poorer. However, the content of Ni_2O_3 is greater and $FeCl_3$ is lower in the sample treated in the autoclave than in atmosphere. The concentrations of Ni_2O_3 and $FeCl_3$ are much less than that of γ-Fe_2O_3, so their magnetization can be neglected in comparison to that of γ-Fe_2O_3. Therefore, the magnetization of the sample treated in atmosphere is higher than that of the sample treated in the autoclave since the larger are the grains, the higher is the magnetization [16].

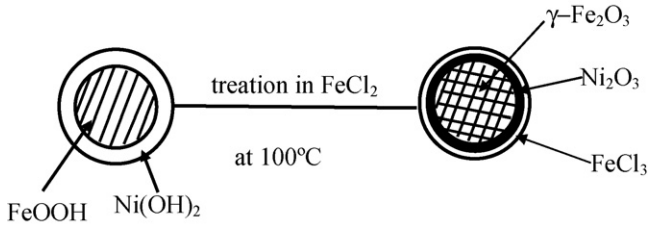

Fig. 4. The schematic model for the distribution of the chemical species of the precursor and nanoparticles prepared by treating in $FeCl_2$ solution at 100 °C.

5. Conclusions

Using a co-precipitation method, a precursor consisting of a composite of amorphous FeOOH and $Ni(OH)_2$ was obtained. The stoichiometric ratio between Ni^{2+} and Fe^{3+} in both the precursor and the calcined sample is in agreement with the ratio in the starting reagents. During the formation of oxide composite nanoparticles, the dissolved $Ni(OH)_2$ can act as a precipitation agent. The transition, in which there is no diffusion of metal ions, is different from the thermally induced transition using calcination and can be denoted as a chemically induced transition. The hydrothermal process is one of the most successful ways to grow crystals of many different materials [17]. The present experimental results indicate that the composite nanoparticles prepared in the autoclave have a similar construction to those prepared in atmosphere though the content of the chemical species is different between the two samples. This means the transition process in the autoclave is same as in the atmosphere. The transition process involves dehydration and crystallization, i.e. $2FeOOH\ (amorph.) \rightarrow \gamma\text{-}Fe_2O_3\ (cryst.) + H_2O$, as well as dehydration and oxidation-crystallization, i.e. $4Ni(OH)_2\ (amorph.) + O_2 \rightarrow 2Ni_2O_3\ (cryst.) + 4H_2O$. The chemically induced transition in $FeCl_2$ solution is also different from the transformation of Fe_3O_4 nanoparticles into $\gamma\text{-}Fe_2O_3$ nanoparticles by oxidation in air [18] or the use of $Fe(NO_3)_3$ solution [19], and the transformation of $ZnFe_2O_4$ nanoparticles into $\gamma\text{-}Fe_2O_3$–$ZnFe_2O_4$ composite nanoparticles by using $Fe(NO_3)_3$ solution [18]. The transition from amorphous hydroxyl to crystallized oxide in $FeCl_2$ solution can provide a new route for the preparation of oxide nanoparticles by co-precipitation.

Acknowledgement

The authors would like to thank Professor Y.M. Huang and Professor C.Z. Huang for fruitful discussions. Financial support for this work was provided by the Nature Science Foundation of China (11074205).

References

[1] S. Sun, Adv. Mater. 18 (2006) 393.
[2] C.-R. Lin, C.-C. Wang, I.-H. Chen, J. Magn. Magn. Mater. 304 (2006) e34.
[3] J. Jiang, Y.M. Yang, Mater. Lett. 61 (2007) 4276.
[4] D.V. Szabo, D. Vollath, Adv. Mater. 11 (1999) 1313.
[5] M. Harada, K. Asakura, N. Toshima, J. Phys. Chem. 98 (1994) 2653.
[6] N. Toshima, M. Harada, T. Yonezawa, K. Kushihaski, K. Asakura, J. Phys. Chem. 95 (1991) 7448.
[7] I.S. Sloufova, B. Vlckova, Z. Basti, T.L. Hasslett, Langmuir 20 (2004) 3407.
[8] N. Toshima, M. Harada, Y. Yamazaki, K. Asakura, J. Phys. Chem. 96 (1992) 9927.
[9] T. Kinoshita, S. Seino, Y. Mizukoshi, T. Nakagawa, T.A. Yamamoto, J. Magn. Magn. Mater. 311 (2007) 255.
[10] H. Yuvaraj, M.H. Woo, E.J. Park, Y.T. Jeong, K.T. Lim, Eur. Polym. J. 44 (2008) 637.
[11] M.D. Butterworth, L. Illum, S.S. Davis, Colloids Surf. A 179 (2001) 93.
[12] X.J. Xu, J. Wang, C.Q. Yang, H.Y. Wu, F.F. Yang, J. Alloys Compd. 468 (2009) 414.
[13] Q. Liu, Z. Xu, J.A. Finch, R. Egerton, Chem. Mater. 10 (1998) 3936.
[14] T. Sato, T. Iijima, M. seki, N. Inagaki, J. Magn. Magn. Mater. 65 (1987) 252.
[15] R. Arulmurugn, G. Vaidyolanthan, S. Sendhilnathan, B. Jeyadevan, Physica B 363 (2005) 225.
[16] Z.X. Tang, C.M. Sorensen, K.J. Klabunde, G.C. Hadjipanayis, J. Appl. Phys. 69 (1991) 5279.
[17] J. Wang, Mater. Sci. Eng. B 127 (2006) 81.
[18] Y.K. Sun, M. Ma, Y. Zhang, N. Gu, Colloids Surf. A 245 (2004) 15.
[19] M.H. Sousa, F.A. Tourinho, J.C. Rubim, J. Raman Spectrosc. 31 (2000) 185.